Collective multipole oscillations direct the plasmonic coupling at the nanojunction interfaces

Nasrin Hooshmand[a,1] and Mostafa A. El-Sayed[a,1]

[a]Laser Dynamics Laboratory, School of Chemistry and Biochemistry, Georgia Institute of Technology, Atlanta, GA 30332

Contributed by Mostafa A. El-Sayed, August 9, 2019 (sent for review June 3, 2019; reviewed by Luis M. Liz-Marzán and Paras N. Prasad)

We present a systematic study of the effect of higher-multipolar order plasmon modes on the spectral response and plasmonic coupling of silver nanoparticle dimers at nanojunction separation and introduce a coupling mechanism. The most prominent plasmonic band within the extinction spectra of coupled resonators is the dipolar coupling band. A detailed calculation of the plasmonic coupling between equivalent particles suggests that the coupling is not limited to the overlap between the main bands of individual particles but can also be affected by the contribution of the higher-order modes in the multipolar region. This requires an appropriate description of the mechanism that goes beyond the general coupling phenomenon introduced as the plasmonic ruler equation in 2007. In the present work, we found that the plasmonic coupling of nearby Ag nanocubes does not only depend on the plasmonic properties of the main band. The results suggest the decay length of the higher-order plasmon mode is more sensitive to changes in the magnitude of the interparticle axis and is a function of the gap size. For cubic particles, the contribution of the higher-order modes becomes significant due to the high density of oscillating dipoles localized on the corners. This gives rise to changes in the decay length of the plasmonic ruler equation. For spherical particles, as the size of the particle increases (i.e., ≥80 nm), the number of dipoles increases, which results in higher dipole–multipole interactions. This exhibits a strong impact on the plasmonic coupling, even at long separation distances (20 nm).

silver nanoparticle pairs | field enhancement | localized surface plasmon resonance | dipole–multipole interaction | plasmonic coupling equation

Metallic nanoparticles made of gold, silver, copper, or aluminum exhibit localized surface plasmon resonance (LSPR) at wavelengths determined by their material properties, shape, and size (1–12). This property makes plasmonic nanoparticles important in many scientific areas, including imaging, plasmonic devices (13), near-field scanning optical microscopy, optical energy transport, and chemical and biological sensing (14–20). The LSPR of a metal nanoparticle is particularly sensitive to the presence of other proximate metal nanoparticles. When coupled nanoparticles are within a few nanometers away from each other, light can be tightly confined to the gaps between the nanoparticles. A dominant dipole feature is observed due to interparticle coupling associated with a strong induced charge in the interparticle gap (21–24). For very small separation, this response becomes weak when the coupling across the ultrathin gap becomes so strong that dipolar oscillations across the coupled resonators are inhibited (25–27). In a previous publication, we studied the effect of changing the interparticle separation on the sensing quality of Au nanocube (AuNC) and Ag nanocube (AgNC) dimers in different surrounding media (28). Using the discrete dipole approximation (DDA), it was observed that the surface plasmon resonance (SPR) is stronger when the 2 nanoparticles are in close proximity to one another and that the distance between the particles has a great effect on the value of the sensitivity factor (1, 21, 22). For metallic nanoparticles with sharp corners, light can be strongly localized even with minimum sizes of 10 to 100 nm (29, 30). We have shown that as the gap size decreases, the redshift becomes singular and dipolar modes determine the coupling between the particles that play a major role in the plasmonic coupling (31). In the present work, we expand our previous study (28, 32, 33), to demonstrate that the plasmonic coupling in dimeric nanoparticles can be predicted not only from the dipole–dipole interaction but also from the interaction between dipole and higher-order plasmonic modes (dipole–multipole, multipole–multipole interactions, etc.), which becomes important to consider as a contribution in the near-field coupling of a pair of plasmonic nanoparticles. It was found that the LSPR peak position of various nanoparticle dimers varied exponentially with the interparticle separation of the dimer (34, 35). In 2007, El-Sayed and coworkers introduced the universal plasmonic ruler equation, which considers the exponential behavior of the dipolar plasmonic coupling of Au nanodiscs having large separation distances (36). In the present work, we include the contribution of shorter-wavelength higher multipolar modes in the plasmonic coupling of coupled Ag nanoparticles by varying the separating distance from 2 to 20 nm. It is found that the interference between the higher-order plasmonic modes in near-field coupling appears at small gap sizes for the nanocubes (37). However, in spherical nanoparticles, the effect of the higher-order modes in plasmonic coupling appears in particles of much larger sizes (80 nm). One important property to understand is how the higher-energy bands can interfere with the near-field coupling when the symmetry changes. Ag has been proposed as a promising candidate among all plasmonic metal nanoparticles to use for studying the effect of high-energy modes in the plasmonic

Significance

We present a systematic study of the effect of higher-multipolar order plasmon modes on the spectral response and plasmonic coupling of Ag nanoparticle dimers at nanojunction separation and introduce a coupling mechanism. It was found that as the interdimer axis decreases, an increase in the plasmon dipolar and multipolar interaction takes place. Further, we found the plasmonic coupling depends on the density of the dipoles on the nanoparticle; as the dipole density increases, the average multipole density increases, resulting in higher dipole–multipole interactions. This study allows us to advance our understanding of the plasmonic response of coupled metal nanoparticles that have not been previously reported and will be useful to drive future experiments to design more sensitive nanoparticle-based sensors.

Author contributions: N.H. and M.A.E.-S. designed research; N.H. performed research; N.H. analyzed data; and N.H. and M.A.E.-S. wrote the paper.

Reviewers: L.M.L.-M., CIC biomaGUNE; and P.N.P., State University of New York at Buffalo.

The authors declare no conflict of interest.

[1]To whom correspondence may be addressed. Email: nhooshmand3@gatech.edu or melsayed@gatech.edu.

This article contains supporting information online at www.pnas.org/lookup/suppl/doi:10.1073/pnas.1909416116/-/DCSupplemental.

First published September 5, 2019.

coupling mechanism, due to its high plasmonic response in the visible region with multiplasmonic bands (35, 38, 39). Previously, we reported the near-field coupling of AgNC dimers in the form of 1-dimensional exponential decay model (32, 33). Herein, we extend our understanding by introducing additional terms in the plasmonic equation, to include the higher-order modes in the near-field coupling of dimeric Ag nanoparticles. We studied the contribution of higher-order modes in the plasmonic coupling between a pair of AgNCs in 2 different orientations. The optical properties and the formation of hot spots between a pair of coupled nanoparticles can be calculated by solving the appropriate Maxwell's equations (40). Using the DDA (41) as a powerful theoretical method, we modeled and calculated the optical properties of a dimer of AgNCs in face-to-face (FF) and edge-to-edge (EE) orientations. In addition, we studied the effect of the shape and size of the nanoparticles on the near-field coupling, by using larger size of the Ag spherical nanoparticles. Varying the separation distance between the nanoparticles and including the higher-order modes in the plasmonic coupling between the nanoparticles, we were able to quantitatively demonstrate the mechanism of plasmonic coupling through the present equations.

Theoretical Method

Using the DDA (41, 42), it is possible to quantitatively investigate the contribution of the higher-order modes in the plasmonic coupling between a pair of Ag nanoparticles (AgNPs). Models were used to investigate the optical properties and interactions between AgNCs with an edge length of 42 nm in water as a medium. It is known that the DDA (41) is one of the most powerful numerical methods of modeling the optical properties of plasmonic nanoparticles (extinction, absorption, and scattering components) with arbitrary geometry. This method includes multipolar and finite size effects. DDA is based on solving Maxwell's equations and has been described in great detail elsewhere (1, 41). The experimental system consists of a pair of AgNPs represented as a cubic array of several thousands of polarizable point dipoles. The point dipoles are excited by an external field, and the response of this excitation to the external field and to other dipole points is solved self-consistently using Maxwell's equations. The size of the nanoparticle is defined by an equal volume of a sphere with an effective radius of $a_{eff} = (3v/4\pi)^{1/3}$. For instance, a_{eff} for the pair of AgNCs (42 nm edge length) is 32.82 nm. The refractive index of the silver nanoparticle is assumed to be the same as that of the bulk metal (43), and water is used as the medium surrounding the cubes, with a refractive index of 1.33. In all cases, the exciting light was polarized parallel to the dimer axis. The plasmonic field enhancement factor (in log scale of $|E|(2)/|E0|(2)$) was calculated using the DDA technique at different excitation wavelengths.

Results and Discussion

Plasmonic Coupling Depends on the Degree of the Oscillating Electron Density. The plasmonic interaction between the AgNCs can be calculated from the shift in the plasmon band maximum that is a function of the interparticle separation distance. The refractive index of the surrounding environment is that of water ($n = 1.33$), and the incident light is polarized along the interparticle axis.

Fig. 1 shows the results of the DDA calculation of the extinction spectra as a function of the wavelength for a dimer of AgNCs in EE and FF orientations with interparticle separations ranging from 2 to 20 nm. In the case of the FF AgNCs dimer, as the 2 nanocubes separate from 2 to 20 nm, the main band continuously shifts to longer wavelengths, and this behavior can be seen in the higher-order mode as well. When the separation distance reaches 2 nm, the higher-order modes clearly dominate over the dipolar modes and have significant dipolar characteristics. This is an elevated interaction with the incident radiation and redshift toward longer wavelengths. This suggests that the effect of the higher-order mode on the plasmonic coupling is more prominent at very short separation distances. One possible explanation for this phenomenon is that when 2 coupled resonators are very close to each other, there are enough multipoles to interact with each other and with dipoles. When the size of multipoles increases, the corresponding band intensity increases (Fig. 1). Moreover, in the FF orientation, there are 2 different states of polarization of the oscillating dipoles extracted from the facing facets and facing corners. These have an additional effect on the LSPR coupling of AgNCs (9), resulting in the main peak (dipolar mode) splitting into 2 peaks. Whereas, for the EE AgNCs, the higher-order mode merged to the dipolar mode and appeared as 1 prominent plasmonic band. Previous results showed that in the EE AgNCs, the extent of the redshift at 2 nm gap size for the multipolar mode is greater than the similar condition in the FF AgNCs (33). There is an increased intensity of the higher-order modes in the extinction spectra of the EE AgNCs (400 to 500 nm) that is not seen in the FF AgNCs (Fig. 1*B*). Field enhancement values, field contour, and vector plots for the FF AgNCs and EE AgNCs in water with light polarized parallel to the interparticle axis are shown in Fig. 2 and *SI Appendix*, Figs. S1 and S2, respectively. The field enhancement trend of the EE AgNCs and FF AgNCs shows for both cases as the separation distance decreases, the maximum field enhancement increases. It can be seen that for all interparticle separations (2, 4, 8, 10, and 20 nm), there is an increase in the field enhancement maximum for EE AgNCs compared to the FF AgNCs under similar conditions (Fig. 2*A* and *SI Appendix*, Figs. S1 and S2). This corresponds to the strong plasmonic coupling between the 2 facing corners, which depends on the higher density of the oscillation electrons

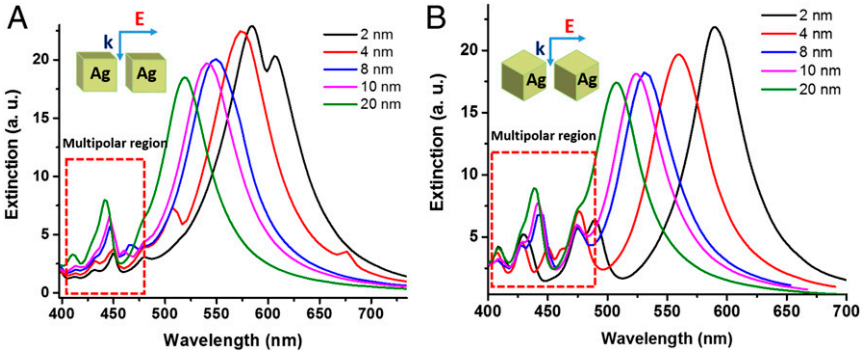

Fig. 1. DDA calculated extinction spectra for the AgNCs in (*A*) FF and (*B*) EE orientations at varying separation distances of the dimer (2, 4, 8, 10, and 20 nm). The incident light is polarized along the interparticle axis.

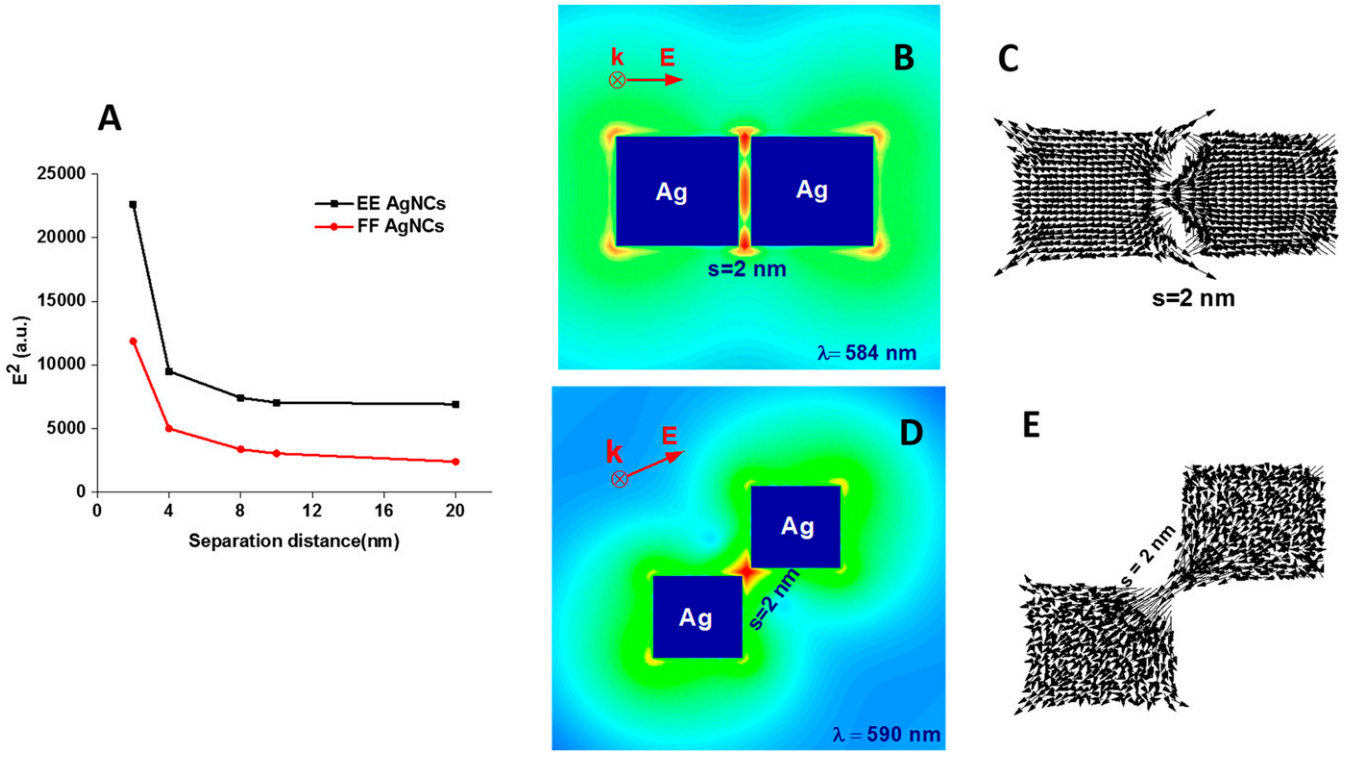

Fig. 2. (*A*) Field enhancement values for the FF AgNCs and EE AgNCs at varying separation distances of the dimer (2, 4, 8, 10, and 20 nm). The wavelength of excitation was chosen based on the peak maximum within extinction spectra in Fig. 1 for each separation distance. (*B–E*) Field contour and polarization vector plots for the dimer of 42 nm FF AgNCs and EE AgNCs at 2 nm separation.

concentrated on the EE AgNCs corners. As noted earlier, an additional feature in the main plasmonic band of the FF AgNCs is split into 2 distinct plasmonic modes at 584 and 606 nm and forms inhomogeneity of the field distribution between both the 2 facing facets and facing corners at very short separation distances (2 nm), that is not present in the EE AgNCs (Fig. 2 *B* and *C*). In larger gaps (>2 nm), the density of the oscillating dipoles and consequence fields strongly are localized around the cube corners (*SI Appendix*, Fig. S1). For the EE AgNCs, there is always only 1 prominent plasmonic band observed. The plasmonic field distribution and the corresponding dipole polarization vectors are more localized around adjacent corners at a short distance (2 nm) (Fig. 2 *D* and *E*).

Contributions of the Dipolar and Multipolar Components in the Plasmonic Coupling Equation. The plasmonic ruler equation is valid for coupled nanoparticles when they are in close proximity to one another (36) and represents only 1 term in the plasmonic coupling equation (i.e., dipolar mode). In the present work, the separation distance between 2 AgNCs was varied from 100 to 2 nm. When the gap size was small enough (~0.05 of the cube size), multipolar modes were allowed take place and interact with each other and with the dipolar mode. In Fig. 3, we introduced a coupling mechanism that includes the contribution of higher-order multipolar modes in the plasmonic coupling regime. The plot shows the fractional plasmonic shift versus the

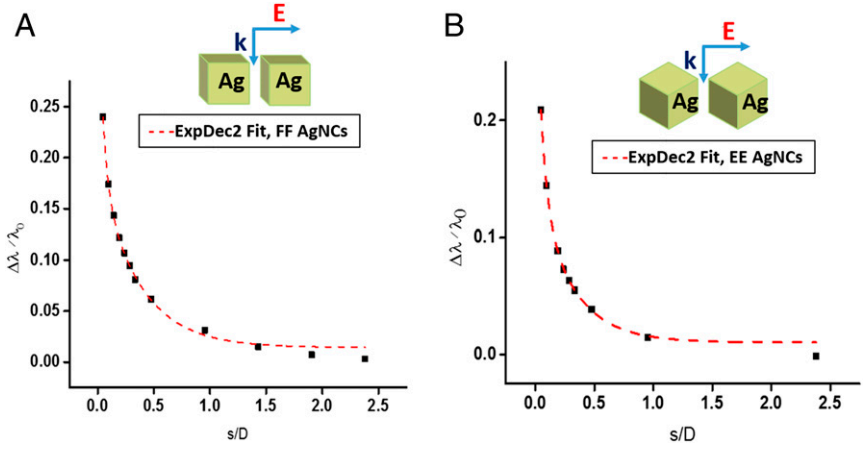

Fig. 3. Dependence of the extinction band maximum shift ($\Delta\lambda/\lambda_0$) as a function of the interparticle separation scaled by either (*A*) the size of the monomer for FF AgNCs or (*B*) the diameter of the monomer for EE AgNCs. The data fit well to the second-order exponential model.

ratio of the interparticle separation scaled by either the length of the single cube for the FF AgNCs or the diameter of the single cube for the EE AgNCs. The presence of each contribution was qualitatively computed from the long separation distance (dipolar mode) and short separation distance components (multipolar mode) by corresponding terms. Eq. **1** describes the plasmonic near-field coupling by an exponential fit, using the exponential function of the form, $\Delta\lambda/\lambda_0 = a.\exp\left(\frac{-s/D}{\tau_1}\right) + b.\exp\left(\frac{-s/D}{\tau_2}\right)$, where the fractional plasmon shift ($\Delta\lambda/\lambda_0$) is a function of the separation distance (normalized to the particle size, s/D) of the dimer: a, b and τ_1, τ_2 are fit parameters that describe the coupled field strength and decay constant, respectively. This approximation indicates that the value of a coupled field strength is 0.2 for the multipolar region and 0.18 for the dipolar region. The decay rates of short distance component ($1/\tau_1$) and long distance component ($1/\tau_2$) were estimated to be 25 and 2.86, respectively, giving an R^2 value of 0.994 for the FF AgNCs. The contribution of the multipolar modes in plasmonic coupling can be calculated by dividing the characteristic values of field strength, yielding a value of 1.11. Therefore, the relative contributions of each term in the plasmonic coupling can be written more accurately as follows:

$$\Delta\lambda \Big/ \lambda_0 = 0.18\exp\left(\frac{-s/D}{0.35}\right) + 0.20\exp\left(\frac{-s/D}{0.04}\right). \quad [1]$$

In a similar condition for EE AgNCs, the relative contributions of each term in the plasmonic coupling are given by

$$\Delta\lambda/\lambda_0 = 0.19exp\left(\frac{-s/D}{0.05}\right) + 0.14exp\left(\frac{-s/D}{0.29}\right), \quad [2]$$

with a coupled field strength of 0.19 and a decay rate of 20 for the contribution of higher-order multipoles and a coupled field strength of 0.14 with a decay rate of 3.4 for the contribution of dipoles. The data fit well to the second-order exponential model, giving an R^2 value of 0.993. The ratio of the higher-order multipole to that of dipole in this equation is 1.36. This implies that the multipolar contribution is slightly higher for the EE AgNCs than for the FF AgNCs (1.36 vs. 1.11). It appears that for both FF and EE AgNCs, there is a long distance component that shows a slow decay rate and a short distance component that shows a fast decay rate. It is possible that the short distance component is representative of dipole–multipole coupling.

Later, we included higher-order resonance terms in the plasmonic coupling. Fig. 4 shows the fractional plasmon shift versus the interparticle distance scaled by either the size of the cube (FF AgNCs) or by the diameter of the cube (EE AgNCs), using the third simultaneously exponential fit. We found a better exponential fit than the previous model with $R^2 = 0.997$ and $R^2 = 0.999$ for the FF and EE AgNCs, respectively. As shown in Fig. 4*B*, the decay rate increases more as the separation distance shortens for the EE AgNCs. This reveals the high density of the dipoles; therefore, the probability of the higher-order mode involved in the plasmonic coupling of the EE AgNCs is greater than the FF AgNCs in a similar condition. This suggests that the contributions of the dipole and the multipolar components are greater in the EE AgNCs. By including more terms (i.e., higher-order resonance modes) in the plasmonic equation, this analysis can be completed, leading to the following equations:

$$\Delta\lambda/\lambda_0 = 0.03\exp\left(\frac{-s/D}{0.2}\right) + 0.08\exp\left(\frac{-s/D}{1.35}\right)0.13\exp\left(\frac{-s/D}{0.20}\right), \quad [3]$$

$$\Delta\lambda/\lambda_0 = 0.16\exp\left(\frac{-s/D}{0.10}\right) + 0.12\exp\left(\frac{-s/D}{0.03}\right)0.09\exp\left(\frac{-s/D}{0.58}\right). \quad [4]$$

The decay rate for the EE AgNCs (9.86, 33.33, and 1.73) is greater than that for the FF AgNCs (4.86, 4.86, and 0.73). The contribution of the short component in the plasmon equation is greater in the EE AgNCs: 1.77 versus 0.5 for the FF AgNCs. This suggests that for the EE AgNCs, the increase of the electron density that is generated on each nanocube results in a multipole that is large enough to contribute to the coupling at larger gap sizes. Therefore, in the EE AgNCs, the high population of the dipoles around the corners gives rise to more contributions of higher-order modes in the plasmonic coupling. Furthermore, as the nanoparticles get closer, they experience an inhomogeneous field, and the dipole selection rules break down; thus, multipolar contributions increase. The higher-order modes do contribute in coupling, but they vanish faster as a pair of resonators separate from each other.

Contribution of the Multipolar Modes in the Plasmonic Coupling of Dimeric Nanospheres. Higher-order multipole contribution to plasmonic coupling has been calculated in AgNCs that are close to one another. To verify the fact that increasing the number of dipoles causes more dipole–multipole interactions, therefore increasing the probability of the higher-order mode in the coupling phenomenon, an investigation of the plasmonic coupling in a pair of

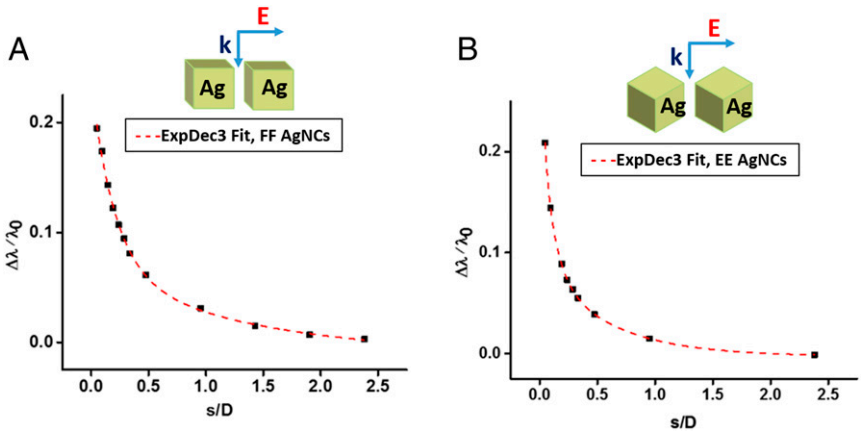

Fig. 4. Dependence of the extinction band maximum shift ($\Delta\lambda/\lambda_0$) as a function of the interparticle separation, which is scaled by either (*A*) the size of the monomer for the FF AgNCs or (*B*) the diameter of the monomer for the EE AgNCs. The data fit well to the third-order exponential model.

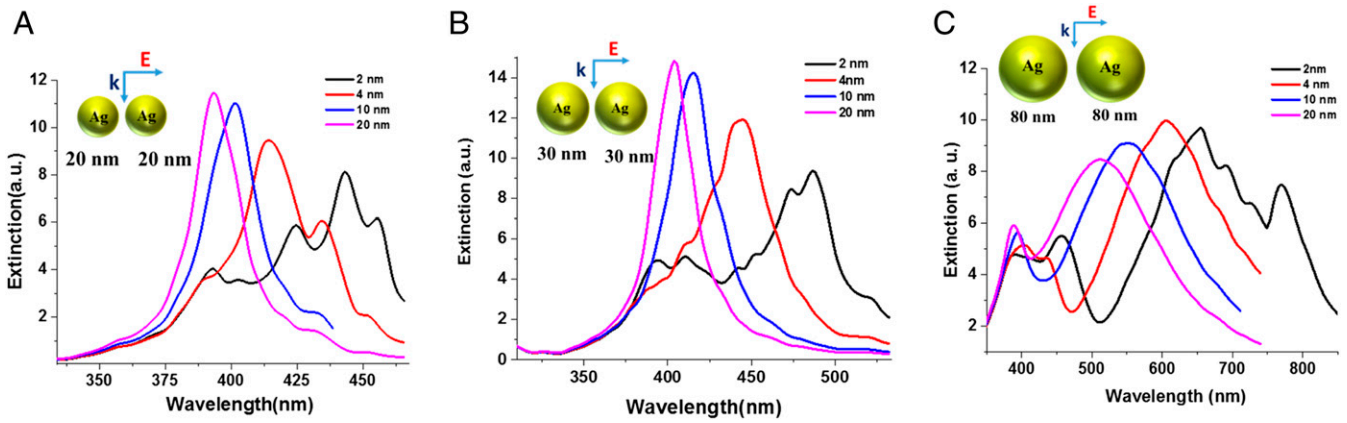

Fig. 5. Calculated extinction spectra for the dimers of AgNSs with a diameter of (*A*) 20 nm, (*B*) 30 nm, and (*C*) 80 nm. The incident light is polarized along the interparticle axis. As the size of the particles increases, this gives rise to largely enhanced interactions between the dipolar and multipolar modes, which can lead to strong coupling, even for large gap sizes (20 nm) for the sphere diameter of 80 nm.

silver nanospheres (AgNSs) has been performed. Fig. 5 shows the extinction spectrum for AgNS dimers, with different sizes (20, 30, and 80 nm) for several values of the relative separation distances. For long separation distances, the dipolar mode (which arises from coupling between dipole modes of each sphere) has a prominent effect on the plasmonic coupling. The results show that for small-sized particles (20 and 30 nm) at a relatively long separation distance (>4 nm), the contribution of multipolar modes in coupling is not noticeable. However, for smaller separation distances (4 and 2 nm), there was a strong population of multipole charges at the gap, resulting in continued redshift of higher multipolar modes, and near-field coupling in the gap was enhanced. It shows multipoles are also important in the interaction between neighboring particles at very small separations and even for small particles. As the size of the particle increases (80 nm), the higher-order modes exhibit a strong impact on the plasmonic coupling, even at a long separation distance (20 nm), and becomes prominent, which shows an increased contribution in plasmonic coupling toward the longer wavelength. When the gap is deeply shortened (4 nm), the contribution of the multipolar modes in plasmonic coupling dramatically changes and plays an important role in the coupling phenomenon.

This observation can be attributed to the fact that for the small spherical particles at long separation distances, the dipole–multipole interaction is not sufficient to be considered in the plasmonic coupling (*SI Appendix*, Fig. S3). However, for larger-sized particles, as the number of dipoles increases, the probability of finding the multipoles' contribution in plasmonic coupling increases (*SI Appendix*, Fig. S4). Therefore, the field across a large nanoparticle becomes inhomogeneous. The resulting field gradient induces multipoles, which are otherwise forbidden in uniform fields. As a result of the above descriptions, it should be considered that not only do very small separations result in dipoles that contributed to the NIR field coupling, but also higher-order multipoles can contribute to this interaction, depending on nanoparticle size and interparticle separation.

Conclusions

In summary, a quantitative study was performed on plasmonic coupling to determine the contribution of higher-order multipolar modes in the plasmon coupling of Ag nanoparticles. The effect of the intensity of the dipoles in producing multipolar modes has been analyzed. Based on the exponential decay approximation, the plasmonic coupling equation has been completed by introducing the contribution of the higher multipolar modes in the plasmonic coupling equation. In general, as the separation between the dimers decreases, an increase in the plasmon dipolar and multipolar interaction takes place, and a redshift of the plasmonic excitation is observed. In cubic nanoparticles, depending on their orientation, the higher-order multipole contributions become more significant, resulting in higher dipole–multipole interactions, and the LSPR shifts become stronger. This essentially means that the higher-order modes determine the coupling between the particles and have a major role to play in the plasmonic coupling at short separation distances. For spherical particles, the contribution of multipolar modes in plasmonic coupling depends on the size of the nanoparticle. Nanoparticles with large size, the higher multipole modes become dominant and result in an increase in the dipole–multipole interactions. This can lead to strong coupling, even for large gap size (20 nm). The plasmonic coupling depends on the density of the dipoles of the nanoparticles; as the dipole density increases, the average multipole density increases, which results in a stronger coupling interaction. This study allows us to advance our understanding of the plasmonic response of coupled resonators that have not been previously reported. These findings will be very useful to drive future experiments to design more sensitive nanoparticle-based sensors.

ACKNOWLEDGMENTS. We acknowledge the Georgia Institute of Technology for providing high-performance computing resources and support. We thank B. T. Draine and P. J. Flatau for use of their DDA Cod DDSCAT 6.1. The financial support of National Science Foundation Division of Chemistry(CHE) Grant 1608801 is greatly appreciated.

1. K. L. Kelly, E. Coronado, L. L. Zhao, G. C. Schatz, The optical properties of metal nanoparticles: The influence of size, shape, and dielectric environment. *J. Phys. Chem. B* **107**, 668–677 (2003).
2. K.-S. Lee, M. A. El-Sayed, Gold and silver nanoparticles in sensing and imaging: Sensitivity of plasmon response to size, shape, and metal composition. *J. Phys. Chem. B* **110**, 19220–19225 (2006).
3. L. M. Liz-Marzán, Tailoring surface plasmons through the morphology and assembly of metal nanoparticles. *Langmuir* **22**, 32–41 (2006).
4. L. J. Sherry *et al.*, Localized surface plasmon resonance spectroscopy of single silver nanocubes. *Nano Lett.* **5**, 2034–2038 (2005).
5. S. Link, Z. L. Wang, M. A. El-Sayed, Alloy formation of gold–silver nanoparticles and the dependence of the plasmon absorption on their composition. *J. Phys. Chem. B* **103**, 3529–3533 (1999).
6. T. R. Jensen, M. D. Malinsky, C. L. Haynes, R. P. Van Duyne, Nanosphere lithography: Tunable localized surface plasmon resonance spectra of silver nanoparticles. *J. Phys. Chem. B* **104**, 10549–10556 (2000).
7. C. L. Haynes, R. P. Van Duyne, Nanosphere lithography: A versatile nanofabrication tool for studies of size-dependent nanoparticle optics. *J. Phys. Chem. B* **105**, 5599–5611 (2001).
8. W. A. Murray, B. Auguié, W. L. Barnes, Sensitivity of localized surface plasmon resonances to bulk and local changes in the optical environment. *J. Phys. Chem. C* **113**, 5120–5125 (2009).
9. N. Hooshmand, J. A. Bordley, M. A. El-Sayed, Are hot spots between two plasmonic nanocubes of silver or gold formed between adjacent corners or adjacent facets? A DDA examination. *J. Phys. Chem. Lett.* **5**, 2229–2234 (2014).
10. E. R. Encina, E. A. Coronado, Plasmon coupling in silver nanosphere pairs. *J. Phys. Chem. C* **114**, 3918–3923 (2010).

11. J. J. Baumberg, J. Aizpurua, M. H. Mikkelsen, D. R. Smith, Extreme nanophotonics from ultrathin metallic gaps. *Nat. Mater.* **18**, 668–678 (2019).
12. B. J. Wiley *et al*., Maneuvering the surface plasmon resonance of silver nanostructures through shape-controlled synthesis. *J. Phys. Chem. B* **110**, 15666–15675 (2006).
13. S. A. Maier, Plasmonics: Metal nanostructures for subwavelength photonic devices. *IEEE J. Sel. Top. Quantum Electron.* **12**, 1214–1220 (2006).
14. B. M. Reinhard, M. Siu, H. Agarwal, A. P. Alivisatos, J. Liphardt, Calibration of dynamic molecular rulers based on plasmon coupling between gold nanoparticles. *Nano Lett.* **5**, 2246–2252 (2005).
15. J. Zhao, X. Zhang, C. R. Yonzon, A. J. Haes, R. P. Van Duyne, Localized surface plasmon resonance biosensors. *Nanomedicine (Lond.)* **1**, 219–228 (2006).
16. C. Xue, Z. Li, C. A. Mirkin, Large-scale assembly of single-crystal silver nanoprism monolayers. *Small* **1**, 513–516 (2005).
17. A. J. Haes, L. Chang, W. L. Klein, R. P. Van Duyne, Detection of a biomarker for Alzheimer's disease from synthetic and clinical samples using a nanoscale optical biosensor. *J. Am. Chem. Soc.* **127**, 2264–2271 (2005).
18. J. A. Dionne *et al*., Localized fields, global impact: Industrial applications of resonant plasmonic materials. *MRS Bull.* **40**, 1138–1145 (2015).
19. J. Song, J. Qu, M. T. Swihart, P. N. Prasad, Near-IR responsive nanostructures for nanobiophotonics: Emerging impacts on nanomedicine. *Nanomedicine (Lond.)* **12**, 771–788 (2016).
20. K. A. Willets, R. P. Van Duyne, Localized surface plasmon resonance spectroscopy and sensing. *Annu. Rev. Phys. Chem.* **58**, 267–297 (2007).
21. N. J. Halas, S. Lal, W.-S. Chang, S. Link, P. Nordlander, Plasmons in strongly coupled metallic nanostructures. *Chem. Rev.* **111**, 3913–3961 (2011).
22. S. Sheikholeslami, Y. W. Jun, P. K. Jain, A. P. Alivisatos, Coupling of optical resonances in a compositionally asymmetric plasmonic nanoparticle dimer. *Nano Lett.* **10**, 2655–2660 (2010).
23. V. Myroshnychenko *et al*., Modelling the optical response of gold nanoparticles. *Chem. Soc. Rev.* **37**, 1792–1805 (2008).
24. C. L. Haynes *et al*., Nanoparticle optics: The importance of radiative dipole coupling in two-dimensional nanoparticle arrays. *J. Phys. Chem. B* **107**, 7337–7342 (2003).
25. S. K. Ghosh, T. Pal, Interparticle coupling effect on the surface plasmon resonance of gold nanoparticles: From theory to applications. *Chem. Rev.* **107**, 4797–4862 (2007).
26. I. Romero, J. Aizpurua, G. W. Bryant, F. J. García De Abajo, Plasmons in nearly touching metallic nanoparticles: Singular response in the limit of touching dimers. *Opt. Express* **14**, 9988–9999 (2006).
27. J. A. Scholl, A. García-Etxarri, A. L. Koh, J. A. Dionne, Observation of quantum tunneling between two plasmonic nanoparticles. *Nano Lett.* **13**, 564–569 (2013).
28. N. Hooshmand, J. A. Bordley, M. A. El-Sayed, Plasmonic spectroscopy: The electromagnetic field strength and its distribution determine the sensitivity factor of face-to-face Ag nanocube dimers in solution and on a substrate. *J. Phys. Chem. C* **119**, 15579–15587 (2015).
29. J. J. Mock, M. Barbic, D. R. Smith, D. A. Schultz, S. Schultz, Shape effects in plasmon resonance of individual colloidal silver nanoparticles. *J. Chem. Phys.* **116**, 6755–6759 (2002).
30. N. Grillet *et al*., Plasmon coupling in silver nanocube dimers: Resonance splitting induced by edge rounding. *ACS Nano* **5**, 9450–9462 (2011).
31. N. Hooshmand, D. O'Neil, A. M. Asiri, M. El-Sayed, Spectroscopy of homo- and heterodimers of silver and gold nanocubes as a function of separation: A DDA simulation. *J. Phys. Chem. A* **118**, 8338–8344 (2014).
32. J. A. Bordley, N. Hooshmand, M. A. El-Sayed, The coupling between gold or silver nanocubes in their homo-dimers: A new coupling mechanism at short separation distances. *Nano Lett.* **15**, 3391–3397 (2015).
33. N. Hooshmand, J. A. Bordley, M. A. El-Sayed, The sensitivity of the distance dependent plasmonic coupling between two nanocubes to their orientation: Edge-to-edge versus face-to-face. *J. Phys. Chem. C* **120**, 4564–4570 (2016).
34. K. H. Su *et al*., Interparticle coupling effects on plasmon resonances of nanogold particles. *Nano Lett.* **3**, 1087–1090 (2003).
35. C. Tabor, R. Murali, M. Mahmoud, M. A. El-Sayed, On the use of plasmonic nanoparticle pairs as a plasmon ruler: The dependence of the near-field dipole plasmon coupling on nanoparticle size and shape. *J. Phys. Chem. A* **113**, 1946–1953 (2009).
36. P. K. Jain, W. Huang, M. A. El-Sayed, On the universal scaling behavior of the distance decay of plasmon coupling in metal nanoparticle pairs: A plasmon ruler equation. *Nano Lett.* **7**, 2080–2088 (2007).
37. E. Ringe *et al*., Unraveling the effects of size, composition, and substrate on the localized surface plasmon resonance frequencies of gold and silver nanocubes: A systematic single-particle approach. *J. Phys. Chem. C* **114**, 12511–12516 (2010).
38. M. G. Blaber, M. D. Arnold, M. J. Ford, A review of the optical properties of alloys and intermetallics for plasmonics. *J. Phys. Condens. Matter* **22**, 143201 (2010).
39. E. C. Hao, G. C. Schatz, R. C. Johnson, J. T. Hupp, Hyper-Rayleigh scattering from silver nanoparticles. *J. Chem. Phys.* **117**, 5963–5966 (2002).
40. G. Mie, Contributions to the optics of diffuse media, especially colloid metal solutions. *Ann. Phys.* **25**, 377–445 (1908).
41. B. T. Draine, P. J. Flatau, Discrete-dipole approximation for scattering calculations. *J. Opt. Soc. Am. A* **11**, 1491–1499 (1994).
42. T. Jensen, L. Kelly, A. Lazarides, G. C. Schatz, Electrodynamics of noble metal nanoparticles and nanoparticle clusters. *J. Cluster Sci.* **10**, 295–317 (1999).
43. P. B. Johnson, R. W. Christy, Optical constants of the noble metals. *Phys. Rev. B* **6**, 4370–4379 (1972).